Supporting Information

Material Dimensionality Effects on Electron Transfer Rates between $CsPbBr_3$ and CdSe Nanoparticles

Alexandra Brumberg,[1] Benjamin T. Diroll,[2] Georgian Nedelcu,[3,4] Matthew E. Sykes,[2] Yuzi Liu,[2] Samantha M. Harvey,[1] Michael R. Wasielewski,[1] Maksym V. Kovalenko,[3,4] and Richard D. Schaller[1,2,*]

[1] Department of Chemistry, Northwestern University, 2145 Sheridan Rd, Evanston, IL 60208, USA

[2] Center for Nanoscale Materials, Argonne National Laboratory, 9700 Cass Ave, Lemont, IL, 60439, USA

[3] Department of Chemistry and Applied Biosciences, ETH Zürich, Vladimir-Prelog-Weg 1-5/10, CH-8093, Zürich, Switzerland

[4] Empa - Swiss Federal Laboratories for Materials Science and Technology, Überlandstrasse 129, CH-8600, Dübendorf, Switzerland

* schaller@anl.gov

1 Contents

2 Experimental Methods 3
3 Calculation of CdSe and $CsPbBr_3$ Solution Concentrations 5
4 TEM Images of Mixed Films 6
5 Verification of the Single Exciton Regime 7
6 Transient Absorption Spectra 8
7 Photoluminescence Excitation (PLE) 9
8 Time-Resolved Photoluminescence of CdSe Emission 11
9 Photoluminescence Data Analysis 12
10 Time-Resolved PL of Redder CdSe QDs 13
11 Electron Transfer (ET) Rates from trPL 15
12 References 18

2 Experimental Methods

Synthesis of CdSe Quantum Dots (QDs). Zinc-blende CdSe QDs were synthesized using an adaptation[1] of a previously published injectionless technique.[2] 186 mg of cadmium acetylacetonate, 12 mg of selenium powder, 25 mL of octadecene, and 1.0 mL of oleic acid were added to a three-neck flask and heated to 120 °C for one hour under vacuum. Then, the solution was heated to 240 °C under nitrogen. Aliquots were extracted from the reaction flask and measured by UV-vis spectroscopy until the first excitonic feature reached 544 nm, at which point the reaction was cooled back to room temperature. The QDs were precipitated by adding isopropanol and then centrifuging and repeating as necessary with hexane and isopropanol. The QDs were then dispersed and stored in hexane.

Synthesis of CdSe Nanoplatelets (NPLs). 5 ML CdSe NPLs were synthesized according to previously published procedures with slight modifications.[3,4] First, a cadmium myristate precursor was prepared by adding 40 mL of 0.05 M cadmium nitrate in methanol to 240 mL of 0.025 M sodium myristate in methanol; the resulting precipitate was washed with methanol and dried under vacuum overnight.

Then, 170 mg of cadmium myristate and 14 mL of octadecene were placed in a three-neck flask and degassed for 30 minutes under vacuum. The solution was then heated under nitrogen to 250 °C, at which point 12 mg of selenium powder (sonicated in 1 mL of octadecene) was rapidly injected. After 60 seconds, 90 mg of finely-ground cadmium acetate was added to the reaction flask, which was maintained at 250 °C for 10 minutes. The reaction was then allowed to cool; when the temperature reached 70 °C, 2 mL of oleic acid and 15 mL of hexane were added. The solution was then centrifuged at 14500 RPM and the resulting pellet was dissolved in 1-methylcyclohexane and filtered through a 0.2 μm PTFE syringe filter.

Synthesis of $CsPbBr_3$ QDs. $CsPbBr_3$ QDs were prepared according to a previously published procedure.[5] First, a solution of cesium oleate was prepared by heating 0.407 g of cesium carbonate (1.25 mmol), 1.25 mL of oleic acid, and 20 mL of octadecene to 120 °C under vacuum for one hour and then to 150 °C under nitrogen until the cesium carbonate was fully dissolved. Before use, the cesium oleate was heated to 100 °C in order to resolubilize the cesium oleate.

Then, 0.069 g of $PbBr_2$ (0.19 mmol) and 5 mL of octadecene were added to a three-neck flask and dried under vacuum for one hour at 120 °C, at which point 0.5 mL of dried oleylamine and 0.5 mL of dried oleic acid were injected. After the $PbBr_2$ had dissolved completely, the temperature was raised to 180 °C and 0.4 mL of cesium oleate was injected. After 5 seconds, the flask was cooled using a water bath. The QDs were then centrifuged and redissolved and stored in toluene.

Synthesis of $CsPbBr_3$ NPLs. $CsPbBr_3$ NPLs were prepared according to a previously published synthesis of $CsPbBr_3$ QDs with major modifications.[5] Briefly, a solution of 61.5 mmolal $PbBr_2$ in mesitylene was obtained after $PbBr_2$, pre-dried oleic acid (0.896 g) and pre-dried oleylamine (0.893 g) were mixed in a 25 mL three-neck flask containing mesitylene (4.32 g). The flask was connected to a Schlenk line, flushed three times at room temperature in order to remove the excess of O_2, and heated to 130 °C. Cesium oleate (0.8 mL) was swiftly injected and the reaction

mixture was immediately cooled down by a water bath. A detailed procedure for the synthesis of the NPLs will be published elsewhere.

Film Preparation. Portions of the stock solutions of $CsPbBr_3$ and CdSe were dried down and then redispersed in either hexanes or methylcyclohexane at the desired concentration of particles. Solutions using a mixture of $CsPbBr_3$ and CdSe in the desired mole ratio were then prepared and mixed using a Vortex mixer. 1-2 μL of each solution was then dropcast on a glass coverslip.

TEM Imaging. TEM images were acquired on a JEOL 2100F operated at 200kV and a Hitachi HT7700 operated at 100 kV.

Spectroscopic Measurements. Static photoluminescence spectra were collected from samples photoexcited by a 35 ps, 405 nm pulsed diode laser through a fiber optic to a thermoelectrically-cooled CCD. Time-resolved measurements were performed on samples photoexcited using the 400 nm, frequency-doubled output of a 35 fs, Ti:sapphire laser operating at 2 kHz. For transient absorption measurements, a small portion of the 800 nm Ti:sapphire output was focused into a sapphire plate to produce a white light probe. The pump repetition rate was reduced to 1 kHz, and single shot spectra were collected and averaged to produce transient absorption data. For photoluminescence measurements, PL was detected using a single-photon sensitive streak camera.

3 Calculation of CdSe and $CsPbBr_3$ Solution Concentrations

The concentration of nanoparticles (NPs) in the stock solutions of CdSe and $CsPbBr_3$ were calculated using Beer's Law, $A = \varepsilon bc$. The absorbance of each solution was measured at 400 nm using a UV-vis spectrophotometer and a 1 mm path length cuvette. The molar absorptivity of the sample at 400 nm, ε_{400}, was calculated according to the formula[6]

$$\varepsilon_{400}\ [\mathrm{M^{-1}\ cm^{-1}}] = \frac{N_A \sigma\ [\mathrm{cm^2}]}{1000 \ln 10} \#(\mathrm{S1})$$

where N_A is Avogadro's number and σ is the absorption cross-section of the material.

The absorption cross-section was measured using transient absorption (TA) spectroscopy with a 400 nm pump wavelength. The TA signal at different pump powers was measured at 6 ns and then fit to $A - B\exp(-\sigma x)$, where x is the pump fluence in photons/cm^2. For the $CsPbBr_3$ QDs, the value was taken from Ref. 7. The absorption cross-sections and corresponding molar extinction coefficients of all of the materials are reported in Table S1.

Table S1. Absorption cross-sections and molar extinction coefficients of CdSe and $CsPbBr_3$ NPs at their peak wavelengths.

Material	**σ (cm^2)**	**ε_{400} (M^{-1} cm^{-1})**
CdSe QDs	2.1×10^{-15}	5.5×10^5
CdSe NPLs	2.3×10^{-14}	6.0×10^6
$CsPbBr_3$ QDs	7.7×10^{-15}	2.0×10^6
$CsPbBr_3$ NPLs	1.4×10^{-14}	3.8×10^6

4 TEM Images of Mixed Films

TEM grids of mixtures of $CsPbBr_3$ and CdSe were prepared to confirm that mixing of $CsPbBr_3$ and CdSe particles actually occurred, as it has been shown that NPs often resist mixing or form superlattices. As shown below in Figure S1, while generally clusters of each material do form, mixing does nevertheless occur with regions existing where particles of one type are surrounded by the other. This was found to be true for all four mixture types.

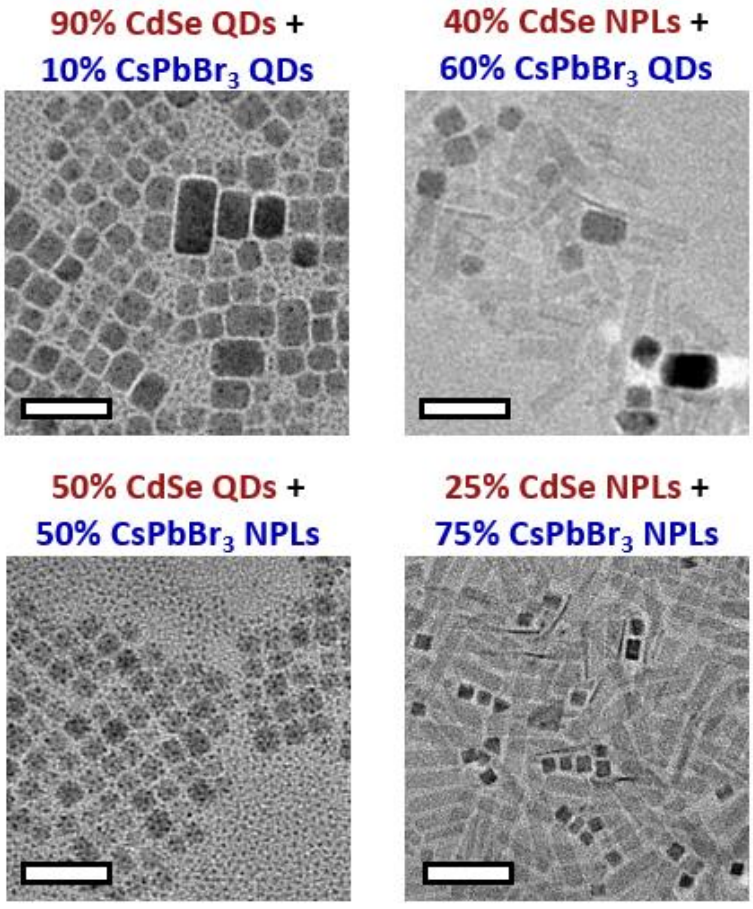

Figure S1. TEM images of mixtures of **(A, C)** CdSe QDs or **(B, D)** CdSe NPLs mixed with either **(A, B)** $CsPbBr_3$ QDs or **(C, D)** $CsPbBr_3$ NPLs. TEM scale bars are all 50 nm.

5 Verification of the Single Exciton Regime

The number of excitons present in each particle is determined by a Poisson distribution,

$$P(k) = \frac{\exp(-\lambda)\,\lambda^k}{k!} \#(S2)$$

where $P(k)$ is the probability that a particle will have k excitons, given an average number of excitons λ. The average number of excitons is typically denoted $\langle N \rangle$ and is given by the formula[8]

$$\langle N \rangle = j_p \sigma \#(S3)$$

where j_p is the pump fluence at 400 nm (in photons/cm^2) and σ is the absorption cross-section (in cm^2). The pump fluence is calculated from the laser spot size and power. Table S2 provides the pump fluences used in the experiments in this work and the values of $\langle N \rangle$ that they correspond to for each material.

Table S2. Pump fluences used in the experiments presented in this work.

Experiment	**Figure**	j_p **(photons/cm^2)**	$\langle N \rangle$
Transient Absorption CdSe NPLs and $CsPbBr_3$ QDs	Figure 2	6.5×10^{12}	CdSe: 0.15 $CsPbBr_3$: 0.05
Time-Resolved Photoluminescence CdSe QDs and $CsPbBr_3$ QDs	Figure 4A	4.5×10^{13}	CdSe: 0.09 $CsPbBr_3$: 0.35
Time-Resolved Photoluminescence CdSe NPLs and $CsPbBr_3$ QDs	Figure 4B	2.5×10^{12}	CdSe: 0.06 $CsPbBr_3$: 0.02
Time-Resolved Photoluminescence CdSe QDs and $CsPbBr_3$ NPLs	Figure 4C	7.3×10^{12}	CdSe: 0.02 $CsPbBr_3$: 0.10
Time-Resolved Photoluminescence CdSe NPLs and $CsPbBr_3$ NPLs	Figure 4D	2.5×10^{12}	CdSe: 0.06 $CsPbBr_3$: 0.04

To verify that the pump fluences given in Table S2 satisfy a single exciton regime in which most of the particles have no excitons and the particles that are excited only have a single exciton, the Poisson distribution for an average number of 0.15 excitons is considered. 86% of particles have zero excitons; the remaining 14% of particles are distributed between mostly single excitons and a small fraction as biexcitons. The number of particles with greater than two excitons is effectively zero.

6 Transient Absorption Spectra

In the main text, Figure 2 shows the bleach of pure CdSe and a film containing both CdSe and $CsPbBr_3$ at 551 nm. The rise of the bleach in the mixed film indicates that the conduction band of CdSe gains electrons (from $CsPbBr_3$) over time. This conclusion is contingent upon the fact that $CsPbBr_3$ does not have any spectral contribution to the TA spectrum of the mixed film at 551 nm. Figure S2 below confirms this.

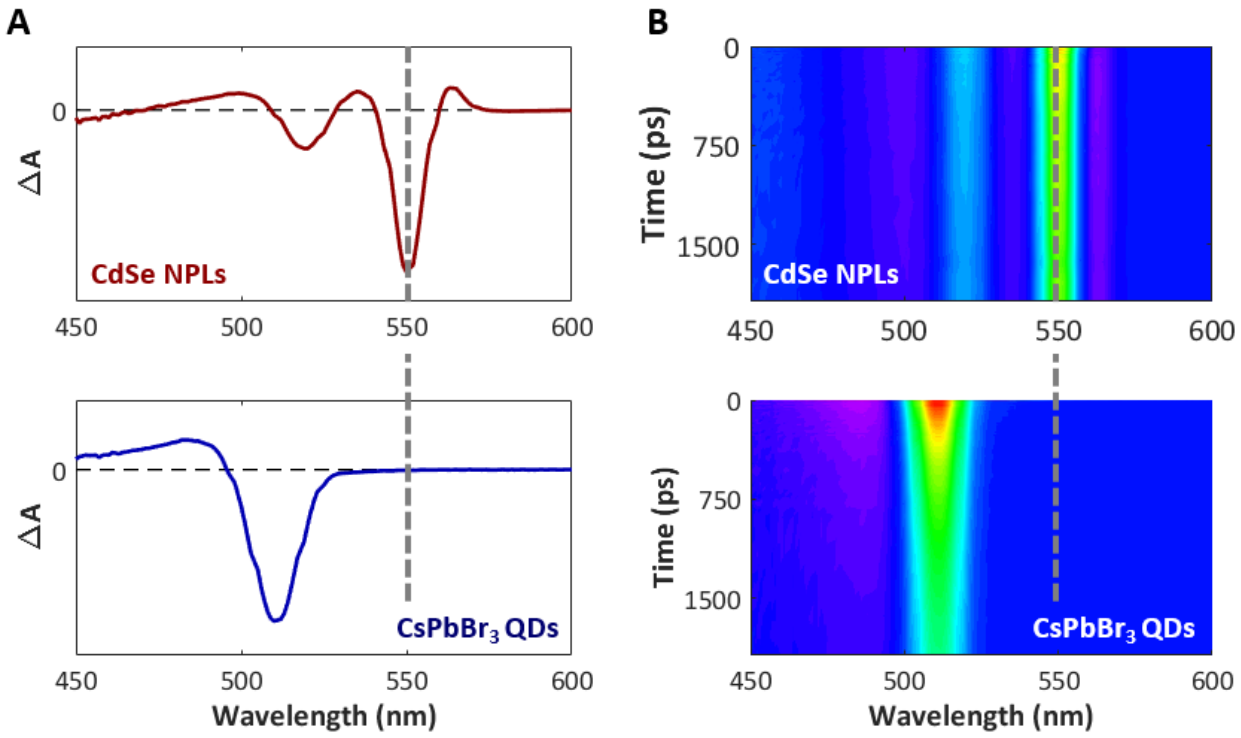

Figure S2. Transient absorption spectra of pure CdSe NPLs and pure $CsPbBr_3$ QDs excited at 400 nm, **(A)** averaged over the ~ 2 ns time window, and **(B)** time-resolved. Note that $CsPbBr_3$ has no spectral feature (neither a photoinduced bleach nor a photoinduced absorption) at 551 nm, the wavelength of the CdSe bleach marked by the dashed line.

This spectral difference is present for both $CsPbBr_3$ QDs and NPLs, as the $CsPbBr_3$ NPLs are located further to the blue (lower in wavelength). For CdSe QDs, some overlap is present between CdSe QDs and $CsPbBr_3$ QDs; however, the low absorption cross-section of CdSe QDs relative to $CsPbBr_3$ (an order of magnitude smaller) makes it difficult to track the bleach of CdSe while still maintaining a low enough fluence for the measurement to be in the single-exciton regime, so no conclusive results were obtained from TA measurements on films containing CdSe QDs.

7 Photoluminescence Excitation (PLE)

Fluorescence resonance energy transfer (FRET) can be confirmed for systems in which energy transfer is possible using photoluminescence excitation (PLE). Since FRET can occur when the emission spectrum of an energy donor overlaps with the absorption spectrum of an energy acceptor, FRET is confirmed by monitoring the emission of the acceptor as a function of excitation wavelength. If the emission of the acceptor increases at excitation wavelengths where the donor absorbs strongly, then the PLE spectrum of the acceptor emission as a function of excitation wavelength will resemble the absorption spectrum of the donor and indicate that FRET does occur. Provided that the absorption spectra of the donor and the acceptor do not overlap, FRET is not present if there is no emission of the acceptor at wavelengths where the donor is excited. Unfortunately, for $CsPbBr_3$ and CdSe, it is not possible to selectively excite $CsPbBr_3$ to monitor potential energy transfer to CdSe; CdSe absorbs light throughout the entirety of the $CsPbBr_3$ absorption spectrum, and so CdSe emission is expected at all wavelengths of the $CsPbBr_3$ absorption spectrum.

A modified approach to the experiment is to monitor the emission of CdSe at various excitation wavelengths and then see if the emission intensity of CdSe resembles that of the absorption spectrum of CdSe added to the absorption spectrum of $CsPbBr_3$ (indicating that it is emitting exactly as much as it would independently, plus even more due to energy transfer from $CsPbBr_3$). The situation is complicated slightly further by the fact that it is not possible to monitor the emission from just CdSe; even at 560+ nm, there is slight emission from the red tail of $CsPbBr_3$. This can be accounted for by fitting the PLE data to extract out the component that arises from CdSe emission.

PLE spectra of $CsPbBr_3$ and CdSe films were collected using a spectrofluorimeter. The samples were excited using a 450 W xenon short-arc lamp and the emission was collected in reflection mode using a photomultiplier tube. The excitation wavelength was scanned from 400 to 572 nm in increments of 4 nm, and the emission intensity from 460 to 600 nm was monitored in increments of 2 nm. The emission from 530 to 600 nm was then fit to a Gaussian (for the CdSe emission) on top of a second-order polynomial (to account for the tail of the $CsPbBr_3$ emission).

Figure S3 shows that when the CdSe PLE emission in a film with a high $CsPbBr_3$ fraction (which increases the likelihood of energy transfer) is compared with the CdSe absorption spectrum, it is lower than expected above 2.6 eV. These results indicate that not only is FRET not happening, but also that $CsPbBr_3$ is a stronger absorber than CdSe—such that the $CsPbBr_3$ particles in the film absorb more of the excitation light than do the CdSe particles. This explains the low CdSe emission at energies above the $CsPbBr_3$ band edge (where $CsPbBr_3$ can absorb light).

It should be noted that an alternative explanation for low emission intensity is that the excitation light provides enough energy to CdSe to induce ionization, thereby also preventing emission from occurring. If this were the case, then low PLE emission intensity would be seen even in PLE spectra of pure CdSe (as opposed to CdSe mixed with $CsPbBr_3$). Previous PLE and

absorption spectra for pure CdSe NPLs do not show significant decreases in PLE emission intensity past 2.6 eV, indicating that the ionization barrier of CdSe NPLs occurs at higher energies than those investigated here.[9]

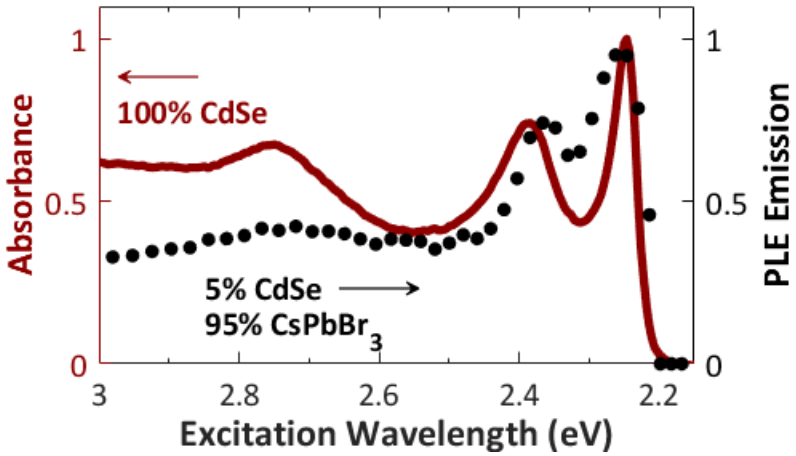

Figure S3. PLE spectrum (black dots) of a film with 5% CdSe NPLs and 95% $CsPbBr_3$ QDs overlaid with the absorption spectrum (dark red line) of neat CdSe NPLs.

8 Time-Resolved Photoluminescence of CdSe Emission

As we note in the main text, trPL of the CdSe emission does not exhibit the slowed decay or rise that would be expected if energy transfer were occuring from $CsPbBr_3$ to CdSe. This can be seen in Figure S4, which shows that indeed, a mixed film containing 55% CdSe NPLs and 45% $CsPbBr_3$ NPLs does not exhibit slowed decay or a rise relative to the neat film of CdSe NPLs. In fact, the mixed film decays more quickly, which can be attributed to hole transfer from CdSe to $CsPbBr_3$. We did not investigate hole transfer as a function of dimensionality, since the lower quantum yield of CdSe relative to $CsPbBr_3$ made it difficult to track the CdSe emission component across multiple films, particularly in the films containing CdSe QDs.

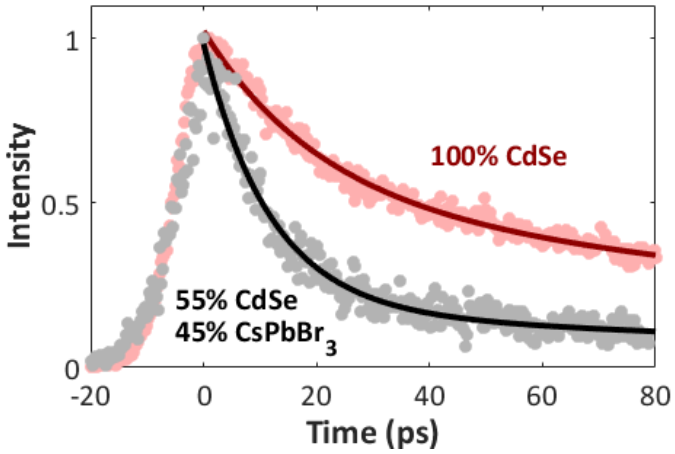

Figure S4. Time-resolved photoluminescence of CdSe NPLs in (red) a neat film of CdSe NPLs versus (black) a mixed film containing 55% CdSe NPLs and 45% $CsPbBr_3$ NPLs. Solid lines are biexponential fits to the data.

9 Photoluminescence Data Analysis

The emission from the $CsPbBr_3$ component of the films containing mixtures of the two materials in static and time-resolved photoluminescence (PL) was analyzed by fitting the spectra of the pure materials to the spectrum of the mixture:

$$\begin{bmatrix} p_1 & c_1 \\ \vdots & \vdots \\ p_m & c_m \end{bmatrix} \begin{bmatrix} tp_1 & \cdots & tp_n \\ tc_1 & \cdots & tc_n \end{bmatrix} = \begin{bmatrix} f_{11} & \cdots & f_{1n} \\ \vdots & \ddots & \vdots \\ f_{m1} & \cdots & f_{mn} \end{bmatrix}$$

where p is the spectrum of pure $CsPbBr_3$, c is the spectrum of pure CdSe, and f is the spectrum of the mixture (static when $n = 1$ and time-resolved when $n > 1$). The weights for p and c as a function of time (or overall, in the case of static PL), tp_i and tc_i, were obtained using matrix division in MATLAB.

It should be noted that the above procedure assumes that the p and c spectra are static and thus do not have dynamics of their own. For time-resolved PL, p and c were determined by taking the sum of the time-resolved spectra over time to obtain a pseudo-static spectrum. For the CdSe QDs and NPLs and $CsPbBr_3$ QDs, the integrated spectrum matched the time-resolved spectra fairly well, and so the assumption that the spectra were static was fairly valid.

For the $CsPbBr_3$ NPLs, the spectra evolve over time; however, the emission of the CdSe NPLs and the $CsPbBr_3$ NPLs are sufficiently spectrally resolved to allow for the dynamics of CdSe and $CsPbBr_3$ to be obtained by spectrally integrating over the peak versus time. This allowed for a comparison of the above approach with one in which the peaks are analyzed via integration, and the two yield essentially identical results. Since the other three series of films exhibited spectral overlap between CdSe and $CsPbBr_3$, their analysis benefited from the approach outlined above.

The dynamics of the $CsPbBr_3$ component (tp_i) are presented in the main text as Figure 4. Only the $CsPbBr_3$ dynamics were analyzed, and all of the fits discussed in the text are of the $CsPbBr_3$ emission.

10 Time-Resolved PL of Redder CdSe QDs

A sample of CdSe QDs with an absorption maximum at 553 nm – essentially isoenergetic with the 552 nm absorption maximum of the CdSe NPLs – were prepared to measure the charge transfer dynamics of QDs with a band gap lower in energy than the band gap of CdSe NPLs (as opposed to the CdSe QDs used in the main text, which have a band gap that is higher in energy). Because the band gap is lower in energy, the conduction band level of these QDs lies lower in energy, thus providing a larger driving force for electron transfer from $CsPbBr_3$ than the other set of CdSe QDs or the CdSe NPLs. The static PL of these CdSe features a primary peak centered at 586 nm with a shoulder at 557 nm. Figure S5 shows the absorption and emission spectra of these "redder" CdSe QDs, as compared to the "bluer" CdSe QDs used in the main text and the CdSe NPLs.

The two sets of CdSe QDs used in this work demonstrate the issues with attempting to produce CdSe QDs isoenergetic with CdSe NPLs. First, only either the absorption or the emission maxima of the QDs and NPLs can be isoenergetic, given that the Stokes shift of CdSe QDs is larger than that of CdSe NPLs. Second, both the absorption and emission peaks in CdSe QDs will be broad, reflecting inhomogeneity in the sample. This inhomogeneity corresponds to a distribution of QD sizes and therefore a distribution of band gaps resulting in varying driving forces for electron transfer.

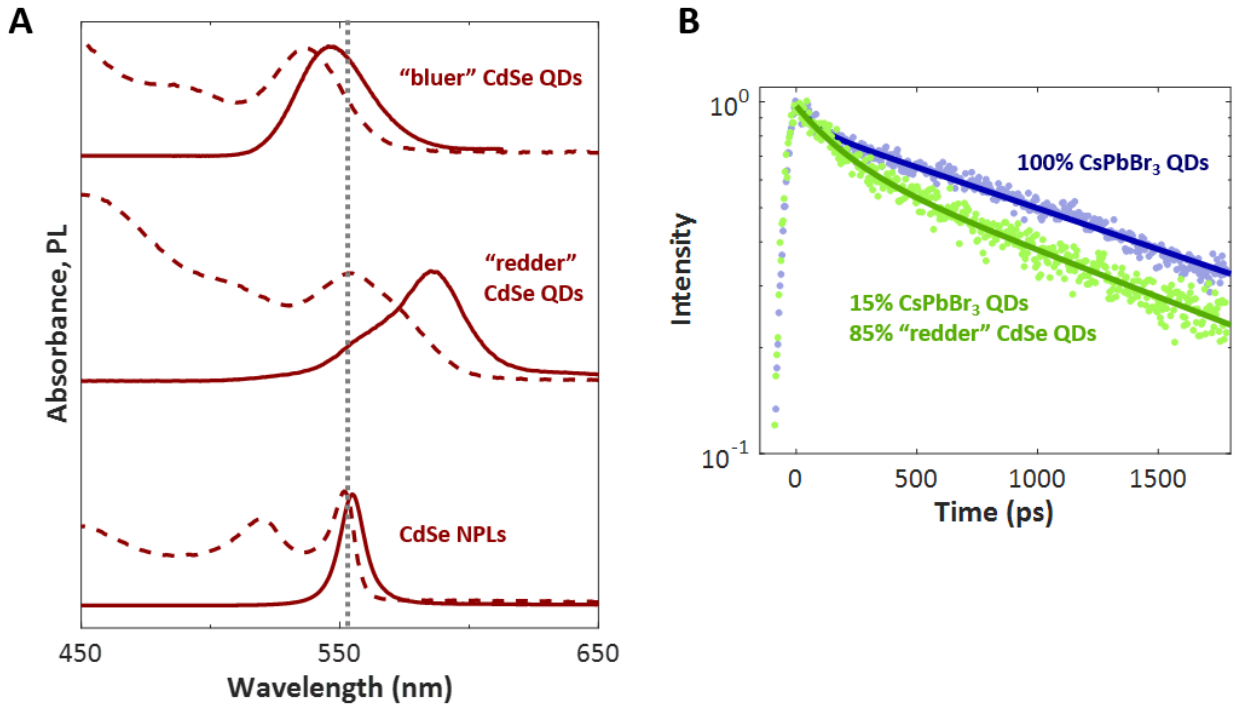

Figure S5. **(A)** Absorption (dashed lines) and photoluminescence (solid lines) spectra of "bluer" and "redder" CdSe QDs as compared to CdSe NPLs. The dotted line marks roughly the wavelength between/near the absorption and emission maxima of the CdSe NPLs. **(B)** Time-resolved PL decay of a film of pure $CsPbBr_3$ QDs and a film of 15% $CsPbBr_3$ QDs and 85%

CdSe QDs. Despite the high fraction of CdSe, the PL decay is not much faster, indicating slow electron transfer.

The time-resolved PL of these redder CdSe QDs mixed with $CsPbBr_3$ QDs confirm that electron transfer is in fact faster for mixtures containing CdSe NPLs than for those containing CdSe QDs, both qualitatively from the lack of significant PL decay and quantitatively from the ET rate of 1.3×10^{-3} ps^{-1} (as compared to 2.2×10^{-3} ps^{-1} for the other CdSe QDs and 3.3×10^{-3} ps^{-1} for the CdSe NPLs, all in mixtures of 85-90% CdSe and 10-15% $CsPbBr_3$ QDs). While in the main text, the CdSe QDs have a slightly lower driving force for electron transfer than the CdSe NPLs, these redder CdSe QDs have a larger driving force for electron transfer and thus should exhibit a faster rate of electron transfer if dimensionality did not play a role. Given that the time-resolved PL decay dynamics of $CsPbBr_3$ in these films containing redder CdSe QDs and $CsPbBr_3$ QDs is still indicative of slow electron transfer, it can be concluded that the higher rates of electron transfer for mixes containing CdSe NPLs derives from the higher dimensionality of the NPLs, rather than any minor difference in driving force.

11 Electron Transfer (ET) Rates from trPL

In the main text, we report the rates of electron transfer for each film, which are calculated using

$$k_{\mathrm{ET}} = \frac{k_{\mathrm{mix}} - (1-x)k_{\mathrm{CsPbBr_3}}}{x} \#(2)$$

where the amplitude-weighted lifetime $\langle\tau\rangle_i = 1/k_i$ is given by

$$\langle\tau\rangle_i = \frac{a_1\tau_1 + a_2\tau_2}{a_1 + a_2}$$

where a_1, a_2, τ_1, τ_2 come from the biexponential fit of each film. The table below provides the amplitude-weighted lifetimes τ_{mix} of each film that were obtained from fitting each decay to a biexponential, as well as $\tau_{\mathrm{CsPbBr_3}}$ for each type of $CsPbBr_3$ NP used in a particular series.

The lifetimes and the parameter x were then used to calculate k_{ET} for each film, reported for each film in Table 1 in the main text. The associated errors with the electron transfer rates can be calculated using the 95% confidence interval on the biexponential fits of the lifetimes and assuming a 5% error in the value of x. In most cases, they are on the order of 10^{-4} ps^{-1}, an order of magnitude lower than the value of the rates.

Typically, in these experiments the spot size used was greater than 600 μm. This larger spot size presented two advantages: (1) A larger spot size makes it easier to ensure low fluence, single exciton dynamics; (2) The larger spot probes a large region of the sample and averages dynamics that might otherwise arise from film inhomogeneity. Nevertheless, to see what role spot-to-spot variability played (if any), we tested four different spots (of maximal separation) on a film containing 25% CdSe QDs and 75% $CsPbBr_3$ NPLs. The spot size was 1 mm and the film diameter was 3 mm. As shown in Figure S6, the four distinct spots exhibited identical dynamics, as would be expected given that a large region of the film is probed each time.

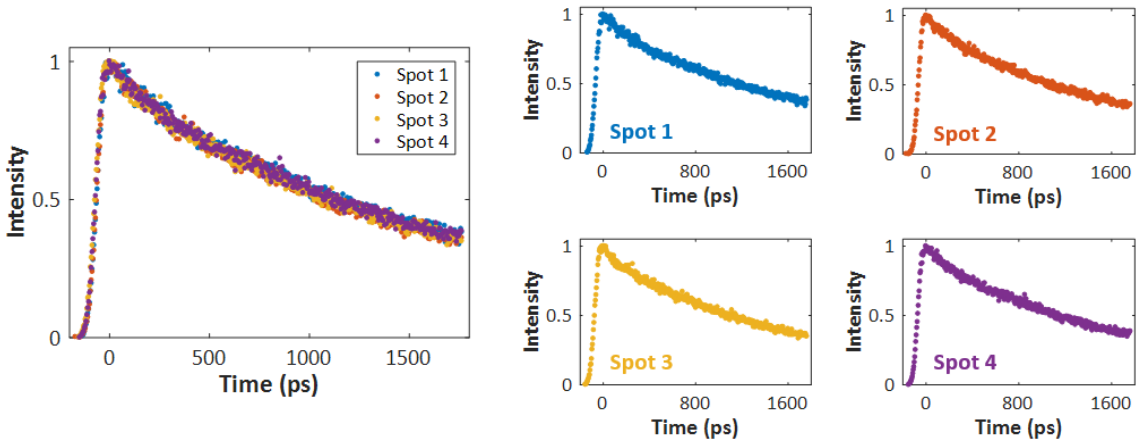

Figure S6. Time-resolved photoluminescence dynamics at four different spots on a film composed of 25% CdSe QDs and 75% $CsPbBr_3$ NPLs.

We note that the reference state for these calculations is the lifetime of the neat films of $CsPbBr_3$. In nanoparticle films (as compared to solutions), self-quenching can be a significant effect, as excitations can migrate between particles in single component solids and find trap states. Introduction of a quencher (such as CdSe) may decrease the effect of such self-quenching. To determine the extent of self-quenching, we compared dynamics in solutions versus films of neat $CsPbBr_3$ NPs using time-resolved photoluminescence.

In neat films, the decay dynamics become just slightly faster compared to those in solutions, as shown below in Figure S7. Here, in order to clearly convey the difference, we plot a linear y-axis. In comparison to the transient photoluminescence data presented in the main text, wherein a CdSe NP quencher is added, self-quenching changes are small in magnitude and comparatively slow. Accounting for the "breaking up" of self-quenching pathways upon addition of CdSe is therefore not significant, and accounting for this would depend upon modeling assumptions, but in the end would not impact the interpretation of our data.

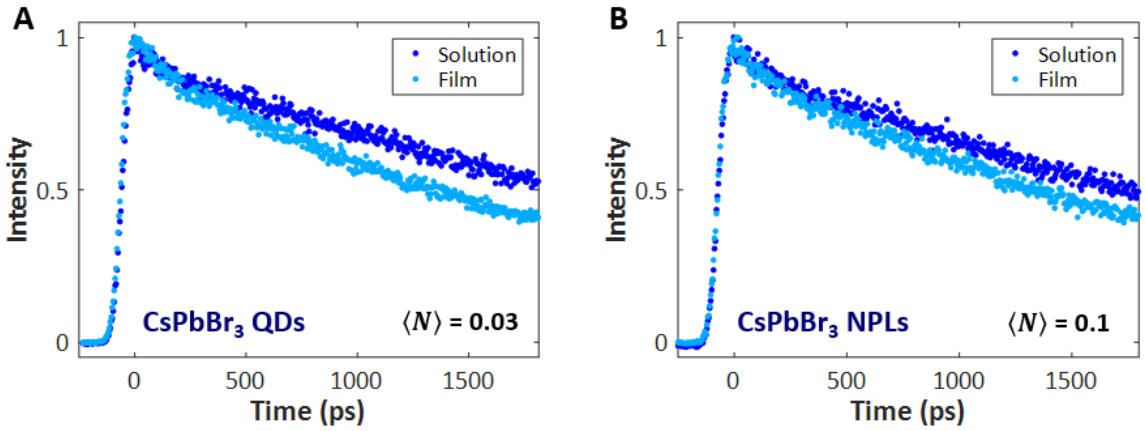

Figure S7. Time-resolved photoluminescence dynamics of $CsPbBr_3$ QDs and NPLs in solutions versus films.

It is also worth noting that for QD donor and molecular acceptor systems, in which acceptors adsorb onto the QD surface, additive kinetics give rise to faster electron transfer rates for higher fractions of acceptors (and thus greater numbers of acceptors bound per QD). The electron transfer rate for when each donor has either 0 or 1 acceptors bound to it, referred to as the bimolecular rate constant, is generally reported as the "true" rate of electron transfer. While the dynamics of charge transfer in films are different than those in solutions, and here we use NPs as both the acceptor and donor, certain aspects still apply. As the fraction of particles that undergo electron transfer increases, so does the rate of electron transfer, despite the fact that the formula to calculate the rate of electron transfer attempts to account for the number of particles that do not undergo charge transfer. However, while in molecular systems the number of adsorbed acceptors (and therefore the instances of charge transfer) can be accounted for using a Poisson distribution, in our films there is no way to quantify the average number of acceptors per donor or use such an average to determine the distribution of numbers of acceptors per donor with Poisson statistics (refer to the TEM images in Figure S1, which show varying numbers of particles surrounding one another).

Table S3. Amplitude-weighted lifetimes ($\langle\tau\rangle_{CsPbBr_3}$ for films with 0% CdSe and $\langle\tau\rangle_{mix}$ for all other films) and fractions of $CsPbBr_3$ particles that underwent electron transfer for all of the films investigated in this work.

Films of CdSe QDs and $CsPbBr_3$ QDs		
% CdSe	**$\langle\tau\rangle$ (ps)**	**x**
0 %	959	-
50 %	830	0.19
80 %	705	0.33
90 %	665	0.40
95 %	543	0.59
99 %	338	0.67

Films of CdSe QDs and $CsPbBr_3$ NPLs		
% CdSe	**$\langle\tau\rangle$ (ps)**	**x**
0 %	2348	-
10 %	1789	0.20
25 %	1639	0.25
50 %	1088	0.53
75 %	730	0.77
90 %	662	0.82

Films of CdSe NPLs and $CsPbBr_3$ QDs		
% CdSe	**$\langle\tau\rangle$ (ps)**	**x**
0 %	1510	-
5 %	1126	0.30
15 %	616	0.68
40 %	554	0.74
65 %	456	0.84
85 %	351	0.84

Films of CdSe NPLs and $CsPbBr_3$ NPLs		
% CdSe	**$\langle\tau\rangle$ (ps)**	**x**
0 %	2227	-
5 %	634	0.80
10 %	632	0.81
25 %	381	0.95
55 %	265	0.98
80 %	183	0.96

12 References

(1) Diroll, B. T.; Fedin, I.; Darancet, P.; Talapin, D. V.; Schaller, R. D. *J. Am. Chem. Soc.* **2016**, *138*, 11109–11112.

(2) Yang, Y. A.; Wu, H.; Williams, K. R.; Cao, Y. C. *Angew. Chem.* **2005**, *44*, 6712–6715.

(3) Ithurria, S.; Dubertret, B. *J. Am. Chem. Soc.* **2008**, *130*, 16504–16505.

(4) She, C.; Fedin, I.; Dolzhnikov, D. S.; Dahlberg, P. D.; Engel, G. S.; Schaller, R. D.; Talapin, D. V. *ACS Nano* **2015**, *9*, 9475–9485.

(5) Protesescu, L.; Yakunin, S.; Bodnarchuk, M. M. I.; Krieg, F.; Caputo, R.; Hendon, C. H.; Yang, R. X.; Walsh, A.; Kovalenko, M. V. *Nano Lett.* **2015**, *15*, 3692–3696.

(6) Jasieniak, J.; Smith, L.; van Embden, J.; Mulvaney, P.; Califano, M. *J. Phys. Chem. C* **2009**, *113*, 19468–19474.

(7) Makarov, N. S.; Guo, S.; Isaienko, O.; Liu, W.; Robel, I.; Klimov, V. I. *Nano Lett.* **2016**, *16*, 2349–2362.

(8) Klimov, V. I.; McBranch, D. W.; Leatherdale, C. A.; Bawendi, M. G. *Phys. Rev. B* **1999**, *60*, 13740–13749.

(9) She, C. X.; Fedin, I.; Dolzhnikov, D. S.; Demortiere, A.; Schaller, R. D.; Pelton, M.; Talapin, D. V. *Nano Lett.* **2014**, *14*, 2772–2777.